Journal of Inorganic Biochemistry 119 (2013) 10–20

Contents lists available at SciVerse ScienceDirect

Journal of Inorganic Biochemistry

journal homepage: www.elsevier.com/locate/jinorgbio

Rhenium(I) tricarbonyl complexes of salicylaldehyde semicarbazones: Synthesis, crystal structures and cytotoxicity

Junming Ho, Wan Yen Lee, Kelvin Jin Tai Koh, Peter Peng Foo Lee, Yaw-Kai Yan *

Natural Sciences and Science Education, National Institute of Education, Nanyang Technological University, 1 Nanyang Walk, Singapore 637616, Singapore

ARTICLE INFO

Article history:
Received 23 July 2012
Received in revised form 10 October 2012
Accepted 23 October 2012
Available online 31 October 2012

Keywords:
Salicylaldehyde semicarbazone
Rhenium(I) carbonyl
Cytotoxicity
Anti-cancer
Crystal structure
Apoptosis

ABSTRACT

A series of *N*,*N*-disubstituted salicylaldehyde semicarbazones (SSCs), $HOC_6H_4CH{=}N\text{-}NHCONR_2$, and their rhenium(I) tricarbonyl complexes, $[ReBr(CO)_3(SSC)]$, have been synthesised and characterised by IR and ^1H NMR spectroscopy. Crystallographic analysis of the complex $[ReBr(CO)_3(H_2Bu_2)]$ (H_2Bu_2 = SSC where R = Bu^n) showed that the SSC acts as a bidentate ligand via its imino nitrogen and carbonyl oxygen atoms. The $[ReBr(CO)_3(SSC)]$ complexes exhibit moderate to high cytotoxicities towards MOLT-4 cells (IC_{50} = 1–24 μM, cf. 18 μM for cisplatin), and the majority of them are virtually non-toxic against non-cancerous human fibroblasts. Apoptotic assays of $[ReBr(CO)_3(H_2Bnz_2)]$ (Bnz = benzyl) revealed that it mediates cytotoxicity in MOLT-4 cells via apoptosis. The complex $[ReBr(CO)_3(H_2Bnz_2)]$ reacts with guanosine by proton transfer from the phenolic OH group to N(7) of guanosine. In $(CD_3)_2SO$, $[ReBr(CO)_3(H_2Bnz_2)]$ undergoes facile conversion to the dimeric complex, $[Re(CO)_3(HBnz_2)]_2$, via bromide dissociation.

1. Introduction

Semicarbazones and thiosemicarbazones (Fig. 1) are versatile compounds that exhibit a wide spectrum of pharmacological activities, including antitumour activity [1–8]. With the increasing interest in metal-based drugs, there is also extensive literature on the medicinal properties of metal complexes of thiosemicarbazones [9–19]. The chemistry and biological activity of semicarbazone complexes have received less attention, however, although the anti-cancer properties of vanadium, iron, copper and platinum complexes of salicylaldehyde semicarbazones have been reported [17,20–22]. Significant cancer cell cytotoxicity has been reported for rhenium(I) tricarbonyl complexes of bis(diphenylphosphinomethyl)amines [23]. Rhenium(I) carbonyl 2-(dimethylamino)ethoxide complexes were also found to be very active against suspended cancer cell lines (e.g. MOLT-4 and HL-60) and solid tumours (e.g. MCF-7 and SK2) [24]. We therefore decided to extend the above studies by investigating the cytotoxicity of rhenium(I) tricarbonyl salicylaldehyde semicarbazone complexes. Whilst rhenium(I) tricarbonyl complexes of thiosemicarbazones are known (but not their biological activity) [25–28], rhenium(I) semicarbazone complexes have not been reported. It is thus also of interest to study the structure and solution chemistry of rhenium(I) salicylaldehyde semicarbazone complexes.

In this paper, we report the synthesis and characterisation of a series of *N*,*N*-disubstituted salicylaldehyde semicarbazones (SSCs) and their rhenium(I) tricarbonyl complexes (Fig. 2). A variety of aliphatic and aromatic *N*-substituents were chosen to generate SSCs and complexes that span a wide range of lipophilicities. The cytotoxicity of these compounds towards two human cancer cell lines (MOLT-4 and MCF-7) and non-cancerous human fibroblasts was also determined. In addition, ^1H NMR experiments were conducted on a representative rhenium complex to investigate its stability in solution and study its reaction with guanosine. This representative rhenium complex was also investigated for its ability to trigger apoptosis in human leukaemia cells (MOLT-4).

2. Experimental

2.1. Materials and apparatus

All experiments were carried out under nitrogen or argon, employing standard Schlenk techniques. Chemical reagents, unless otherwise stated, were used directly from commercial sources. Solvents were dried and distilled under nitrogen before use. The compound $[ReBr(CO)_5]$ was prepared according to a published method [29]. Proton NMR spectra were recorded on a Bruker CRX400 spectrometer at 25 °C. Elemental analyses were carried out using an Elementar Vario MICRO CUBE instrument. The IR spectra were recorded on KBr discs using a Perkin–Elmer Spectrum 100 FT-IR spectrometer.

2.2. Preparation of SSC ligands

The preparative protocol was adapted from published methods [21,30]. For H_2Hex_2, H_2Bnz_2 and H_2Ph_2, the carbamic chloride

* Corresponding author. Tel.: +65 6790 3813; fax: +65 6896 9414.
E-mail address: yawkai.yan@nie.edu.sg (Y.-K. Yan).

0162-0134/$ – see front matter © 2012 Elsevier Inc. All rights reserved.
http://dx.doi.org/10.1016/j.jinorgbio.2012.10.011

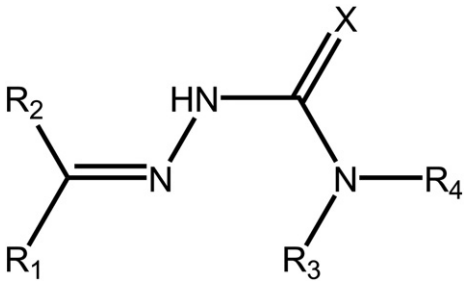

Fig. 1. The general structure of semicarbazones (X = O) and thiosemicarbazones (X = S); R_1, R_2, R_3 and R_4 = H, alkyl or aryl groups.

$[R_2NC(O)Cl]$ was synthesised from the respective amines, whilst for the other ligands, the carbamic chlorides were obtained commercially.

(a) Preparation of carbamic chlorides
A solution of the secondary amine (15 mmol) in dichloromethane (25 mL) was added dropwise via a cannula to a stirred solution of triphosgene (5.25 mmol) and pyridine (30 mmol) in dichloromethane (25 mL) in an ice-water bath. The resultant orange solution was left to stand at room temperature for three days under nitrogen to give a yellow solution of the carbamic chloride.

(b) Preparation of SSCs
To the solution of carbamic chloride was added diethyl ether (60 mL). The resultant mixture was added dropwise to a solution of hydrazine monohydrate (60 mmol) in ethanol (30 mL), with vigorous stirring. The reaction mixture was left to stir for 30 min before the solvents were removed under reduced pressure. The residue was extracted three times with dichloromethane (10 mL each) and the combined extract was evaporated under reduced pressure to give the semicarbazide $[R_2NC(O)NHNH_2]$. A solution of the semicarbazide in toluene (5 mL) was placed on a magnetic stirrer. To this was added an equimolar amount of salicylaldehyde and catalytic amounts of *p*-toluenesulfonic acid. The mixture was stirred at room temperature for 30 min to give a yellow or white precipitate of the semicarbazone, which was isolated by filtration. After washing with cold toluene and drying *in vacuo*, the product was recrystallised from acetone–water mixture.

2.2.1. Data for H_2Bu_2

Yield: (3.3 g, 76%). Anal. Calc. for $C_{16}H_{25}N_3O_2$: C, 65.9; H, 8.7; N, 14.4. Found C, 65.7; H, 8.5; N, 14.5. IR (cm^{-1}): ν(C=O) 1640 vs. ^{1}H NMR [$(CD_3)_2CO$, ppm]: 11.80 (1H, s, phenol O–H), 9.65 (1H, s, hydrazine N–H), 8.28 (1H, s, imine C–H), 7.24 (2H, m, Ph-H), 6.87 (2H, m, Ph-H), 3.37 (4H, t, J = 7 Hz, α-CH_2), 1.61 (4H, m, β-CH_2), 1.35 (4H, m, γ-CH_2), 0.95 (6H, t, J = 6 Hz, CH_3).

2.2.2. Data for H_2Hex_2

Yield: (3.4 g, 65%). Anal. Calc. for $C_{20}H_{33}N_3O_2$: C, 69.1; H, 9.6; N, 12.1. Found C, 69.2; H, 9.4; N, 12.3. IR (cm^{-1}): ν(C=O) 1636 vs. ^{1}H NMR [$(CD_3)_2CO$, ppm]: 11.80 (1H, s, phenol O–H), 9.70 (1H, s, hydrazine N–H), 8.27 (1H, s, imine C–H), 7.23 (2H, m, Ph-H), 6.88 (2H, m, Ph-H), 3.37 (4H, t, J = 7 Hz, α-CH_2), 1.63 (4H, m, β-CH_2), 1.33 (12H, m, γ- to ε-CH_2), 0.90 (6H, t, J = 6 Hz, CH_3).

2.2.3. Data for H_2Bnz_2

Yield: (4.0 g, 75%). Anal. Calc. for $C_{22}H_{21}N_3O_2$: C, 73.6; H, 5.9; N, 11.6. Found C, 73.7; H, 6.3; N, 11.6. IR (cm^{-1}): ν(C=O) 1645 vs. ^{1}H NMR [$(CD_3)_2SO$, ppm]: 11.55 (1H, s, phenol O–H), 10.85 (1H, s, hydrazine N–H), 8.35 (1H, s, imine C–H), 7.2-7.4 (12H, m, Ph-H), 6.88 (2H, m, Ph-H), 4.52 (4H, s, CH_2).

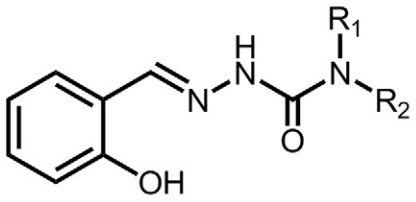

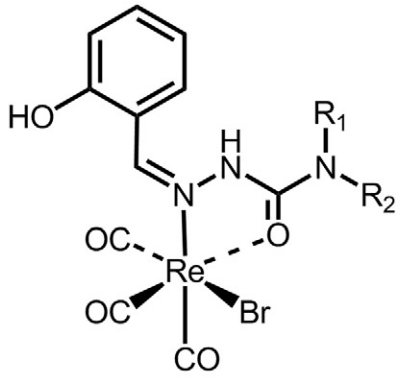

Ligand	R_1	R_2
H_2Bu_2	butyl	butyl
H_2Hex_2	hexyl	hexyl
H_2Bnz_2	benzyl	benzyl
H_2MePh	methyl	phenyl
H_2Ph_2	phenyl	phenyl
H_2BF	NR_1R_2 = 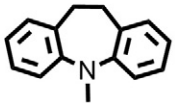	

Fig. 2. The salicylaldehyde semicarbazones and rhenium(I) carbonyl complexes synthesised in this work.

2.2.4. Data for H_2MePh

Yield: (2.4 g, 60%). Anal. Calc. for $C_{15}H_{15}N_3O_2$: C, 66.9; H, 5.6; N, 15.6. Found C, 66.9; H, 5.9; N, 15.4. IR (cm^{-1}): ν(C═O) 1661 vs. ^{1}H NMR [$(CD_3)_2CO$, ppm]: 11.65 (1H, s, phenol O–H), 9.35 (1H, s, hydrazine C–H), 8.10 (1H, s, imine C–H), 7.1–7.5 (7H, m, Ph-H), 6.82 (2H, m, Ph-H), 3.31 (3H, s, CH_3).

2.2.5. Data for H_2Ph_2

Yield: (3.0 g, 60%). Anal. Calc. for $C_{20}H_{17}N_3O_2$: C, 72.2; H, 5.1; N, 12.9. Found C, 72.3; H, 5.3; N, 12.7. IR (cm^{-1}): ν(C═O) 1691 vs. ^{1}H NMR [$(CD_3)_2CO$, ppm]: 11.58 (1H, s, phenol O–H), 9.61 (1H, s, hydrazine N–H), 8.18 (1H, s, imine C–H), 7.1–7.5 (12H, m, Ph-H), 6.84 (2H, m, Ph-H).

2.2.6. Data for H_2BF

Yield: (4.3 g, 81%). Anal. Calc. for $C_{22}H_{19}N_3O_2$: C, 73.9; H, 5.4; N, 11.8. Found C, 73.7; H, 5.6; N, 11.6. IR (cm^{-1}): ν(C═O) 1655 vs. ^{1}H NMR [$(CD_3)_2SO$, ppm]: 11.45 (1H, s, phenol O–H), 10.10 (1H, s, hydrazine N–H), 8.32 (1H, s, imine C–H), 7.42 (2H, m, Ph-H), 7.27 (8H, m, Ph-H), 6.87 (2H, m, Ph-H), 3.08 (4H, s, CH_2).

2.3. Preparation of [ReBr(CO)$_3$(SSC)] complexes

A mixture of [$ReBr(CO)_5$] (0.2 mmol), SSC (0.2 mmol) and toluene (3 mL) was placed in a Schlenk tube with a magnetic stirrer bar. The mixture was refluxed and the progress of the reaction was monitored hourly by IR spectroscopy. For the H_2Hex_2 ligand, the reaction mixture was stirred at 105 °C, slightly below the boiling point of toluene, because decomposition occurred at refluxing temperature. Generally, the reaction was complete after 5 h.

Some the complexes (where L = H_2Bu_2, H_2Bnz_2 and H_2MePh) began to precipitate out within the first 2 h of reaction. For these complexes, the crude product was isolated by filtration and washed with a small volume of cold toluene. The crude product was dissolved in a minimum amount of dichloromethane and layered with hexane to afford yellow crystals within three days.

In other cases (L = H_2Hex_2, H_2Ph_2 and H_2BF), the crude product was obtained as a waxy solid by removing the toluene under reduced pressure. Recrystallisation was carried out by dissolving the solid in a minimum amount of dichloromethane and mixing with approximately two volumes of hexane to form a homogeneous solution. The vial was sealed with sealing film and stored at 8 °C for three days to obtain yellow crystals of the complex. The crystals were washed with a small volume of hexane, crushed and dried under reduced pressure.

2.3.1. Data for [ReBr(CO)$_3$(H_2Bu_2)]

Yield: (58 mg, 45%). Anal. Calc. for $C_{19}H_{25}BrN_3O_5Re$: C, 35.6; H, 3.9; N, 6.6. Found C, 35.3; H, 3.9; N, 6.4. IR (cm^{-1}): ν(C≡O) 2028 vs, 1914 vs, 1902 vs; ν(C═O) 1625 s. ^{1}H NMR [$(CD_3)_2CO$, ppm]: 8.30(1H, s, imine C–H), 7.75 (1H, m, Ph-H), 7.55 (1H, m, Ph-H), 7.22 (1H, d, J = 8 Hz, Ph-H), 7.15 (1H, t, J = 8 Hz, Ph-H), 3.40 (4H, m, α-CH_2), 1.64 (4H, m, β-CH_2), 1.37 (4H, m, γ-CH_2), 0.94 (6H, t, J = 6 Hz, CH_3).

2.3.2. Data for [ReBr(CO)$_3$(H_2Hex_2)]

Yield: (59 mg, 42%). Anal. Calc. for $C_{23}H_{33}BrN_3O_5Re$: C, 39.6; H, 4.8; N, 6.0. Found C, 39.6; H, 4.9; N, 6.1. IR (cm^{-1}): ν(C≡O) 2029 vs, 1930 vs, 1887 vs; ν(C═O) 1626 s. ^{1}H NMR [$(CD_3)_2CO$, ppm]: 8.30(1H, s, imine C–H), 7.75 (1H, m, Ph-H), 7.55 (1H, m, Ph-H), 7.17 (2H, m, Ph-H), 3.44 (4H, m, α-CH_2), 1.67 (4H, m, β-CH_2), 1.35 (12H, m, γ- to ε-CH_2), 0.89 (6H, t, J = 6 Hz, CH_3).

2.3.3. Data for [ReBr(CO)$_3$(H_2Bnz_2)]

Yield: (57 mg, 40%). Anal. Calc. for $C_{25}H_{21}BrN_3O_5Re$: C, 42.3; H, 3.0; N, 5.9. Found C, 42.4; H, 3.1; N, 5.9. IR (cm^{-1}): ν(C≡O) 2030 vs, 1923 vs, 1878 vs; ν(C═O) 1616 s. ^{1}H NMR [$(CD_3)_2SO$, ppm]: 7.86(1H, s, imine C–H), 7.2-7.4 (12H, m, Ph-H), 6.85 (1H, d, J = 8 Hz, Ph-H), 6.69 (1H, t, J = 8 Hz, Ph-H), 4.64 (2H, br d, J = 16 Hz, CH_2), 4.43 (2H, br d, J = 16 Hz, CH_2).

2.3.4. Data for [ReBr(CO)$_3$(H_2MePh)]

Yield: (50 mg, 40%). Anal. Calc. for $C_{18}H_{15}BrN_3O_5Re$: C, 34.9; H, 2.4; N, 6.8. Found C, 34.9; H, 2.4; N, 6.8. IR (cm^{-1}): ν(C≡O) 2025 vs, 1916 vs, 1881 vs; ν(C═O) 1626 vs. ^{1}H NMR [$(CD_3)_2CO$, ppm]: 8.25(1H, s, imine C–H), 7.4–7.6 (7H, m, Ph-H), 7.04 (1H, m, Ph-H), 6.95 (1H, m, Ph-H), 3.47 (3H, m, CH_3).

2.3.5. Data for [ReBr(CO)$_3$(H_2Ph_2)]

Yield: (49 mg, 36%). Anal. Calc. for $C_{23}H_{17}BrN_3O_5Re$: C, 40.5; H, 2.5; N, 6.1. Found C, 40.3; H, 2.6; N, 5.9. IR (cm^{-1}): ν(C≡O) 2027 vs, 1920 vs, 1889 vs; ν(C═O) 1618 m. ^{1}H NMR [$(CD_3)_2CO$, ppm]: 8.34 (1H, s, imine C–H), 7.3-7.6 (12H, m, Ph-H), 7.05 (1H, m, Ph-H), 6.93 (1H, m, Ph-H).

2.3.6. Data for [ReBr(CO)$_3$(H_2BF)]

Yield: (78 mg, 55%). Anal. Calc. for $C_{25}H_{19}BrN_3O_5Re$: C, 42.4; H, 2.7; N, 5.9. Found C, 42.1; H, 2.9; N, 5.9. IR (cm^{-1}): ν(C≡O) 2028 vs, 1915 vs, 1892 vs; ν(C═O) 1623 m. ^{1}H NMR [$(CD_3)_2CO$, ppm]: 10.77 (1H, s, hydrazine N–H), 8.31(1H, s, imine C–H), 7.3-7.7 (10H, m, Ph-H), 7.02 (1H, m, Ph-H), 6.92 (1H, m, Ph-H), 3.5 (4H, s, CH_2).

2.4. Formation of [Re(CO)$_3$($HBnz_2$)]$_2$ and [Re(CO)$_3$($HHex_2$)]$_2$

Hexane was layered over dilute solutions of the mononuclear complexes, [$ReBr(CO)_3(H_2Bnz_2)$] and [$ReBr(CO)_3(H_2Hex_2)$], respectively, in dichloromethane. Crystals of the corresponding dinuclear complexes, [$Re(CO)_3(HBnz_2)]_2$ and [$Re(CO)_3(HHex_2)]_2$, were formed after two weeks at room temperature.

2.4.1. Data for [Re(CO)$_3$($HBnz_2$)]$_2$

IR (cm^{-1}): ν(C≡O) 2021 vs, and 1902 vs; ν(C═O) 1573 s. ^{1}H NMR [$(CD_3)_2SO$, ppm]: 12.40 (2H, s, hydrazine N–H), 7.91 (4H, d, J = 9 Hz, Ph-H), 7.88 (2H, s, imine C–H), 7.4-7.2 (20H, m, Ph-H), 6.78 (4H, q, J = 9 Hz, Ph-H), 4.55 (8H, q, J = 16 Hz, CH_2).

2.4.2. Data for [Re(CO)$_3$($HHex_2$)]$_2$

IR (cm^{-1}): ν(C≡O) 2018 vs, 1910 vs, and 1879 vs; ν(C═O) 1585 m. ^{1}H NMR ($CDCl_3$, ppm): 13.83 (2H, s, hydrazine N–H), 7.82 (2H, s, imine C–H), 7.50 (2H, m, Ph-H), 7.1–7.3 (4H, m, Ph-H), 6.82 (2H, m, Ph-H), 3.65 (2H, m, α-CH_2), 3.0–3.3 (4H, m, α-CH_2), 2.55 (2H, m, α-CH_2), 1.46–1.06 (32H, m, β- to ε-CH_2), 0.96–0.84 (12H, m, CH_3).

2.5. X-ray crystallography

Crystals of [$ReBr(CO)_3(H_2Bu_2)$] were grown by layering hexane over a dilute solution of the complex in dichloromethane. Single crystals of [$Re(CO)_3(HBnz_2)]_2$ and [$Re(CO)_3(HHex_2)]_2$ were obtained as described in Section 2.4. The crystals were mounted on glass fibres for data collection at 298(2) K. The data were collected in the θ/2θ mode using a Siemens P4 diffractometer with Mo Kα radiation (λ = 0.71073 Å), and were corrected for absorption effects using ψ-scan data. The structures were solved by the heavy atom method and refined by full-matrix least-squares on F^2. All non-hydrogen atoms were refined anisotropically. Hydrogen atoms were introduced in calculated positions and allowed to ride on their carrier atoms. Crystal and refinement data are given in Table 1.

The carbon atoms C(17), C(18), C(19) and C(18′) of [$ReBr(CO)_3(H_2Bu_2)$] showed very large displacement parameters, suggesting disorder. Refinement was performed with two disordered positions (65% and 35% occupancies, respectively) for each of these atoms, with the

disordered butyl chains being restrained to have C – C bond lengths of 1.5400 ± 0.0001 Å. The C – C – C angles involving the disordered atoms are restrained to be 109.50 ± 0.01°. Adjacent carbon atoms of each disordered chain are restrained to have similar U_{ij} components, allowing for a gradual change in magnitude and direction of the anisotropic displacement parameters from the α-carbon outward.

The hexyl chains of $[Re(CO)_3(HHex_2)]_2$ were restrained to have C – C bond lengths of 1.5400 ± 0.0001 Å and C – C – C angles of 109.50 ± 0.01°. Adjacent carbon atoms of each chain are restrained to have similar U_{ij} components, allowing for a gradual change in magnitude and direction of the anisotropic displacement parameters from the α-carbon outward.

2.6. Cell types and culture conditions

The human cancer cell lines, MOLT-4 (T-lymphoblastic leukaemia) and MCF-7 (breast carcinoma), were obtained from the American Type Culture Collection. Human foreskin fibroblasts (as a passage 1 culture) were obtained from the Department of Surgery, National University of Singapore. Growth of the fibroblasts was subsequently expanded and a passage 4 culture was used for the cytotoxicity assay. An RPMI-1640 based medium containing 10% foetal bovine serum was used to culture MOLT-4 cells, while Dulbecco's Minimal Essential Medium/Ham's F12 medium (1:1) supplemented with 10% foetal bovine serum was used for MCF-7 cells. Human fibroblasts were cultured in Dulbecco's Minimal Essential Medium supplemented with 20% foetal bovine serum. All media also contained 100 units/mL of penicillin and 100 μg/mL of streptomycin. The cells were maintained at 37 °C in a 5% CO_2 incubator.

2.7. Cytotoxicity assay

Cytotoxicity of the compounds was determined using the MTT [3(3,4-dimethylthiazol-2-yl)-2,5-diphenyltetrazolium bromide] assay [31] on microtitre plates. The suspended MOLT-4 cells were seeded at 40,000 cells per well and exposed to compounds on the same day, while the adherent MCF-7 cells and fibroblasts were seeded at 20,000 cells per well and cultured for 24 h prior to treatment with compounds.

All compounds were dissolved in absolute DMSO at a concentration of 100 mM. These solutions were then diluted to various concentrations, using a 10% v/v solution of DMSO in the appropriate culture medium, before being added to the cell culture wells. The final DMSO concentration was 1.25% v/v in each well. Six serial dilutions were made for each compound in order to generate a dose–response curve, and six replicate wells were set up for each concentration of the compound. Each plate contained a blank well (cell-free medium-only well), solvent control wells which contained cells and 1.25% v/v DMSO, drug colour control wells which contained drug and medium only, and growth control wells which contained only cells in medium.

Following incubation of cells with test fractions for 24 h at 37 °C and 5% CO_2, 20 μL of a 5 mg/mL solution of MTT was added to each well (final MTT concentration 1 mg/mL). Three hours later, 100 μL of lysing solution (20% sodium dodecyl sulfate dissolved in 50% *N*, *N*-dimethylformamide, pH adjusted to 4.7 with acetic acid) was added to each well. After the microtitre plate was left to stand overnight, the absorbance of the solution in each well was read at 570 nm. The percent inhibition of growth for each concentration of compound was calculated from the absorbance [31] and plotted against the concentration to give a graph from which the IC_{50} value (concentration of compound required to inhibit the growth of the cells by 50%) was determined.

Table 1
Crystallographic data and structure refinement details for $[ReBr(CO)_3H_2Bu_2]$, $[Re(CO)_3(HBnz_2)]_2$ and $[Re(CO)_3(HHex_2)]_2$.

Complex	$[ReBr(CO)_3(H_2Bu_2)]$	$[Re(CO)_3(HBnz_2)]_2$	$[Re(CO)_3(HHex_2)]_2$
Chemical formula	C_{19} H_{25} Br N_3 O_5 Re	C_{50} H_{40} N_6 O_{10} Re_2	C_{46} H_{64} N_6 O_{10} Re_2
Formula weight	641.53	1257.28	1233.44
Crystal system	Monoclinic	Monoclinic	Triclinic
Space group	P2(1)/n	C2/c	P−1
a (Å)	12.525(4)	19.281(5)	10.031(2)
b (Å)	19.21(1)	13.684(3)	10.3750(9)
c (Å)	19.297(5)	17.610(2)	13.953(1)
α (°)	90	90	108.958(5)
β (°)	94.68(2)	99.31(1)	109.44(1)
γ (°)	90	90	93.310(9)
Volume (Å^3)	4627(4)	4585(2)	1272.5(3)
Z	8	4	1
Crystal size (mm^3)	0.30×0.20×0.10	0.30×0.20×0.10	0.30×0.20×0.10
θ Range (°)	1.87 to 25.01	1.83 to 25.00	2.11 to 25.00
Max. and min. transmission	0.9835 and 0.4515	0.8037 and 0.5103	0.9301 and 0.6603
μ (mm^{-1})	7.012	5.343	4.810
Reflections collected	9893	4832	5199
Independent reflections	8093 [R(int) = 0.0384]	4030 [R(int) = 0.0299]	4375 [R(int) = 0.0223]
Final R indices [I>2sigma(I)]	R_1 = 0.0495, wR_2 = 0.0974	R_1 = 0.0322, wR_2 = 0.0804	R_1 = 0.0378, wR_2 = 0.1004
R indices (all data)	R_1 = 0.1075, wR_2 = 0.1119	R_1 = 0.0436, wR_2 = 0.0851	R_1 = 0.0461, wR_2 = 0.1044

2.8. Assessment of apoptosis induction

The ability of $[ReBr(CO)_3(H_2Bnz_2)]$ to induce apoptosis in MOLT-4 cells was determined by the following experiments. Each experiment was carried out three times to ensure the reproducibility of results.

2.8.1. Annexin V-FITC staining assay

MOLT-4 cells (10^6 for each experiment) were grown in 5 cm^2 sterile petri dishes and treated with $[ReBr(CO)_3(H_2Bnz_2)]$ (7.3 μM) or solvent control (1% DMSO) for 3, 6, 12 and 24 h, respectively. Apoptotic cell death was determined by staining treated cells with Annexin-V-FITC and counterstaining with propidium iodide (PI). Annexin-V-FITC binds to the exposed phosphatidylserine (PS) on the outer plasma membrane of apoptotic cells, while PI is excluded by viable cells with intact membranes. Cells positive for annexin-V-FITC but negative for PI are defined as apoptotic, while cells stained with PI alone is indicative of necrosis [32,33]. Treated cells were washed twice with PBS, stained with annexin-V-FITC (BD Pharmingen, 51-65874X) and PI (Sigma, 20 μg/mL), and analysed on a Dako Cytomation Cyan LX flow cytometer with 488 nm laser excitation. Emission from FITC was detected at 525 nm and that for PI at 575 nm.

2.8.2. Detection of caspase 3 activity

The caspase 3 activity was quantified according to instructions of the colorimetric assay kit (Clontech 636217). MOLT-4 cells (10^6 for each experiment) were treated with $[ReBr(CO)_3(H_2Bnz_2)]$ (7.3 μM) or solvent control (1% DMSO) for various durations, after which the cells were collected by centrifugation at 200 g for 5 min. The cell pellet was lysed in 50 μL cell lysis buffer. Aliquots of 50 μL of cell lysate were mixed with 50 μL of reaction buffer and incubated with the caspase 3 substrate Ac-DEVD-pNA (50 μM) at 37 °C for 1 h. The caspase 3 activity was determined spectrophotometrically at 405 nm.

2.8.3. Western blot analysis

MOLT-4 cells (10^6 for each experiment) were incubated with $[ReBr(CO)_3(H_2Bnz_2)]$ (7.3 μM) for various durations, after which the cell pellet was collected by centrifugation at 200 g for 5 min at 4 °C. The cells were lysed by resuspension in lysis solution (7 M urea, 2 M thiourea, 4% CHAPS, 30 mM Tris, pH 9.0) and brief sonication on ice for 2 min at 30% amplitude, 30 s intervals. The cell lysates

were centrifuged at 200 g for 5 min, after which the protein-containing supernatants were quantified using the Bradford protein assay reagent (Biorad, 500–0201). Equal amounts of proteins (20 μg) were boiled at 100 °C with 10 μL of 2× Laemmli sample buffer (Biorad, 161–0737) for 2 min, and loaded into each lane of a SDS-PAGE gel (5% stacking, 10% resolving). After electrophoresis, the separated proteins were transferred to a nitrocellulose membrane (GE Healthcare, RPN2020D). The blots were blocked in phosphate buffered saline (PBS) containing 0.05% Tween 20 and 5% non-fat milk for 1 h at room temperature. After blocking, the blots were probed with rabbit polyclonal caspase 3 antibody at 1:2500 dilution (US Biological, C2087-16). After washing twice with PBS Tween (PBS containing 0.05% Tween 20), the blots were incubated with horseradish peroxidase-conjugated polyclonal goat anti-rabbit secondary antibody (1:5000, US Biological, 11904-39) for 1 h at room temperature. Blots were washed again (3×5 min) in PBS Tween and visualised using an enhanced chemiluminescence kit (GE healthcare, RPN2124), in accordance with the manufacturer's recommendations.

3. Results and discussion

3.1. Syntheses

The synthetic protocol for SSCs reported by Lee [14] was modified to improve the efficiency of reaction between the semicarbazide and salicylaldehyde. In Lee's procedure, this reaction was carried out in ethanol at 0 °C, and the SSC product precipitated from the solution. Some of the SSCs used in this work are quite soluble in ethanol, however, and did not precipitate out even after a significant portion of ethanol was evaporated off. This resulted in poor yields for these ligands (<50%). A protocol by Noblia [21] was thus used, in which the reaction between the semicarbazide and salicylaldehyde was carried out in the presence of catalytic amounts *p*-toluenesulfonic acid in toluene at room temperature. Carrying out the reaction at room temperature rather than in an ice-bath also increased the rate of reaction, and the crude product usually precipitated out of solution almost instantaneously. This approach resulted in significantly higher yields (at least 60%) for all the SSCs.

The rhenium(I) tricarbonyl complexes of the SSCs were prepared by refluxing an equimolar mixture of the ligand and $[ReBr(CO)_5]$ in toluene. Toluene was used because it is a non-coordinating solvent with high boiling point. Coordinating solvents such as tetrahydrofuran were found to compete with the SSCs for complexation and resulted in poor yields of the desired complexes.

During an attempt to grow single crystals of the complexes $[ReBr(CO)_3(H_2Bnz_2)]$ and $[ReBr(CO)_3(H_2Hex_2)]$, crystals of the dinuclear complexes $[Re(CO)_3(HBnz_2)]_2$ and $[Re(CO)_3(HHex_2)]_2$ were obtained instead (Fig. 3). These crystals were grown under conditions similar to those for recrystallising the mononuclear complexes, but more dilute solutions were used and consequently crystals only appeared after approximately two weeks. Crystallographic analysis (vide infra) revealed that the phenolic oxygen atoms have been deprotonated, and have displaced the bromide ligands of the rhenium centres to form a bridged structure.

The facile formation of these dinuclear complexes is somewhat unexpected since the soft rhenium(I) centre is expected to bind more strongly to bromide than to the phenoxide oxygen. Presumably, the formation of $[Re(CO)_3(HBnz_2)]_2$ and $[Re(CO)_3(HHex_2)]_2$ is driven by entropy rather than enthalpy, with the formation of 2 mol of gaseous HBr contributing to the increase in entropy. The reaction most likely proceeds via the dissociation of bromide as the rate-limiting step, followed by coordination of the hydroxyl group, and then deprotonation. That bromide dissociation is rate-limiting is supported by the fact that, whereas only 50% of $[ReBr(CO)_3(H_2Bnz_2)]$ is converted to $[Re(CO)_3(HBnz_2)]_2$ after 24 h at 37 °C in $(CD_3)_2SO$ (see Section 3.6), quantitative conversion occurs within 30 min after addition of one molar equivalent of $AgNO_3$ to $[ReBr(CO)_3(H_2Bnz_2)]$ at ambient temperature (as shown by ^1H NMR spectroscopy). Carballo et al. have observed the similar formation of a dinuclear $[ReL(CO)_3]_2$ complex during slow concentration of an acetone solution of $[ReBr(CO)_3(HL)]$ (HL = ferrocenylcarbaldehyde N-methylthiosemicarbazone) [27], in which case deprotonation occurs at the hydrazidic nitrogen and Re-S-Re bridges are formed.

3.2. Infrared spectroscopy

All the SSCs synthesised show an intense ν(C═O) absorption band at 1636–1691 cm^{-1}. The carbonyl stretching frequencies are consistently higher for the SSCs bearing aromatic substituents on the terminal nitrogen (H_2Ph_2, H_2MePh and H_2BF). This may be rationalised in terms of resonance effects (Scheme 1), where the phenyl ring stabilises resonance structure III by competing with the carbonyl group for conjugation with the amidic nitrogen lone pair.

The carbonyl stretching frequencies decrease on coordination of the SSCs to rhenium (Table 2). This can be attributed to the stabilisation of resonance structures IIa and IIb through stabilisation of the negative charge on the carbonyl oxygen by the Lewis-acidic rhenium centre. Amongst the complexes, there is negligible difference between the ν(C═O) of the SSC ligands with aliphatic substituents and that of the SSCs with aromatic substituents. This implies that resonance structures IIa and IIb are much preferred over III in the complexes. Interestingly, the C═O stretching frequencies of $[Re(CO)_3(HBnz_2)]_2$ and $[Re(CO)_3(HHex_2)]_2$ are each lower than those of $[ReBr(CO)_3(H_2Bnz_2)]$ and $[ReBr(CO)_3(H_2Hex_2)]$, respectively, by ca. 40 cm^{-1}. Presumably, the phenoxide oxygen, being a poorer σ-donor than bromide, makes the rhenium atoms in the dinuclear complexes more Lewis-acidic than those in the mononuclear complexes, thereby further favouring resonance structures IIa and IIb.

3.3. Proton NMR spectroscopy

The signals of the SSC protons generally shift downfield on coordination. A single imine proton peak appears in the spectrum of each complex, indicating that the SSC ligand is coordinated to the rhenium atom in a single configuration. Interestingly, the methylene protons of the H_2Bnz_2 ligand give two broad doublets in the spectrum of $[ReBr(CO)_3(H_2Bnz_2)]$, as opposed to a sharp singlet in the spectrum

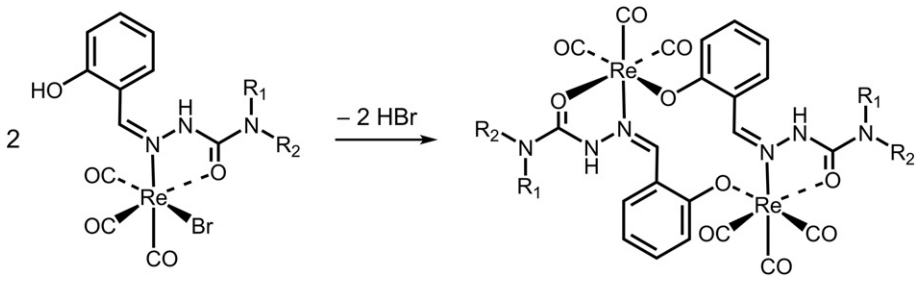

Fig. 3. Formation of the dinuclear complexes $[Re(CO)_3(HBnz_2)]_2$ and $[Re(CO)_3(HHex_2)]_2$.

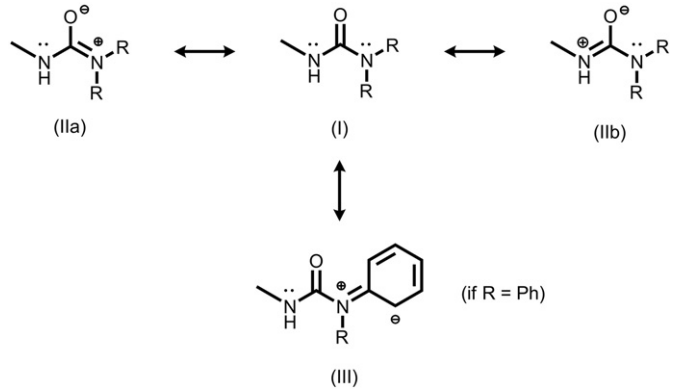

Scheme 1. Four of the resonance structures of the carbamide group of semicarbazones.

Table 2
Comparison of carbonyl stretching frequencies ($\tilde{\nu}$/cm^{-1}) between SSCs and [ReBr(CO)$_3$(SSC)] complexes.

Ligand	$\tilde{\nu}$ (ligand)	$\tilde{\nu}$ (complex)	$\tilde{\nu}$ (ligand)–$\tilde{\nu}$ (complex)
H_2Bu_2	1640	1625	15
H_2Hex_2	1636	1626	10
H_2Bnz_2	1645	1616	29
H_2MePh	1661	1626	35
H_2Ph_2	1691	1618	73
H_2BF	1655	1623	32

of the free ligand. This may be attributed to the stabilisation of resonance structure IIa on complexation (see Section 3.2), which results in hindered rotation of the Bnz_2N-CO bond and hence non-equivalence of the methylene protons. Similar effects are observed in the methylene proton signals of [ReBr(CO)$_3$(H_2Hex_2)] and [ReBr(CO)$_3$(H_2Bu_2)].

3.4. Crystal structures

3.4.1. Crystal structure of [ReBr(CO)$_3$(H_2Bu_2)]

There are two independent molecules of the complex [ReBr(CO)$_3$(H_2Bu_2)] in the unit cell (Fig. 4). The H_2Bu_2 ligand acts as a bidentate ligand, binding to the rhenium centre via the imine nitrogen and carbonyl oxygen. This binding mode to the {Re(CO)$_3$} unit is analogous to that of thiosemicarbazones, wherein the sulfur and imine nitrogen atoms are coordinated to rhenium [25,26,28]. The lengths of the C═O, C═N and C–N bonds within the H_2Bu_2 ligand (Table 3) are similar to those observed in the parent salicylaldehyde

Table 3
Selected bond lengths (Å) and angles (°) for [ReBr(CO)$_3$(H_2Bu_2)].

Bond lengths			
Re(1)-C(1)	1.90(1)	Re(1′)-C(1′)	1.89(1)
Re(1)-C(2)	1.90(1)	Re(1′)-C(2′)	1.89(1)
Re(1)-C(3)	1.90(1)	Re(1′)-C(3′)	1.91(1)
Re(1)-Br(1)	2.615(1)	Re(1′)-Br(1′)	2.627(1)
Re(1)-N(1)	2.167(7)	Re(1′)-N(1′)	2.172(7)
Re(1)-O(5)	2.160(6)	Re(1′)-O(5′)	2.138(6)
C(10)-N(1)[a]	1.28(1)	C(10′)-N(1′)[a]	1.28(1)
C(11)-O(5)[b]	1.25(1)	C(11′)-O(5′)[b]	1.25(1)
C(11)-N(3)[c]	1.32(1)	C(11′)-N(3′)[c]	1.33(1)
C(11)-N(2)[d]	1.37(1)	C(11′)-N(2′)[d]	1.37(1)
Bond angles			
C(11)-N(3)-C(12)	119.9(9)	C(11′)-N(3′)-C(12′)	118.7(8)
C(11)-N(3)-C(16)	123.6(8)	C(11′)-N(3′)-C(16′)	123.8(7)
C(12)-N(3)-C(16)	116.5(7)	C(12′)-N(3′)-C(16′)	117.4(7)

[a] Imine C═N.
[b] Amide C═O.
[c] Amide C–N.
[d] Hydrazide C–N.

semicarbazone, $HOC_6H_4CH{=}N-NHCONH_2$ [34]. The three angles about the terminal nitrogen atom of both molecules in the unit cell [N(3) and N(3′)] sum up to 360°, indicating a trigonal planar geometry for the nitrogen atoms. This is consistent with the dominance of resonance structure IIa (Scheme 1), where the terminal nitrogen is sp^2 hybridised. The chelate rings are virtually planar, with maximum deviations of 0.01 [for C(11)] and 0.03 Å [for N(1′) and N(2′)] from the respective mean planes. The coordination plane of each terminal nitrogen is almost parallel to the mean plane of the chelate ring to which the nitrogen is attached (angles of deviation are 3° each), providing further evidence for the conjugation of the nitrogen lone pair with the C═O double bond. Notably, an intramolecular hydrogen bond exists between the phenolic oxygen and the hydrazine NH group of each molecule (Fig. 4). This is made possible by the adoption of the *cis* configuration by the imine group in the complex (as opposed to the *trans* configuration expected for the free ligand [34]). The imine groups are not coplanar with the phenyl rings bearing them, thus the imino protons deviate significantly from the mean planes of the phenyl rings [by 0.30 Å for the proton on C(10) and 0.29 Å for that on C(10′)]. The Re-Br, Re-CO and Re-NC(imine) distances are close to those observed in analogous rhenium(I) tricarbonyl complexes [25,26,28].

3.4.2. Crystal structures of [Re(CO)$_3$($HBnz_2$)]$_2$ and [Re(CO)$_3$($HHex_2$)]$_2$

The deprotonated SSC ligands adopt a tridentate coordination mode in [Re(CO)$_3$($HBnz_2$)]$_2$ (Fig. 5) and [Re(CO)$_3$($HHex_2$)]$_2$ (Fig. 6), with the imine nitrogen and carbonyl oxygen binding to one rhenium

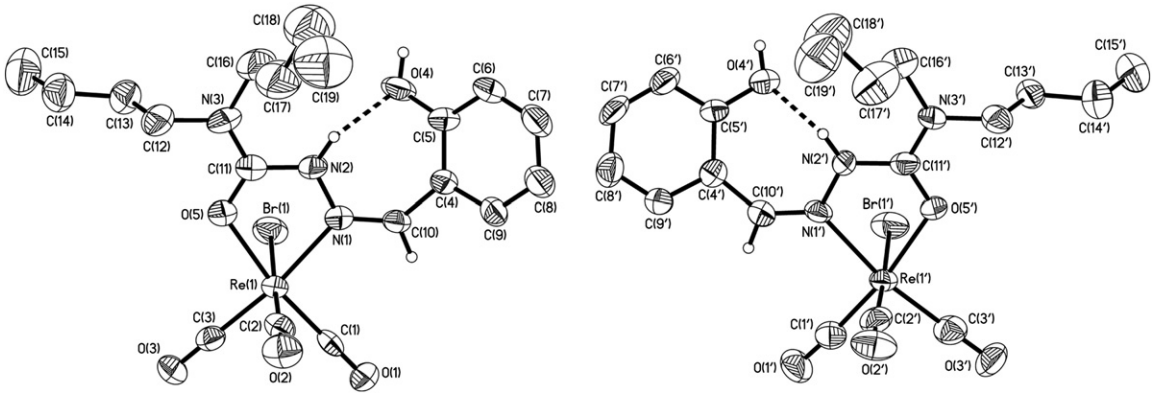

Fig. 4. The two independent molecules in the crystal structure of [ReBr(CO)$_3$(H_2Bu_2)] (40% probability ellipsoids); hydrogen atoms bonded to the butyl and phenyl groups are omitted for clarity. An intramolecular hydrogen bond exists between O(4) and N(2) and between O(4′) and N(2′) [O(4)···H(2A) 1.98 Å, O(4)···N(2) 2.64 Å, ∠O(4)···H(2A)-N(2) 133°; O(4′)···H(2′A) 2.03 Å, O(4′)···N(2′) 2.65 Å, ∠O(4′)···H(2′A)-N(2′) 128°, N–H 0.860 Å].

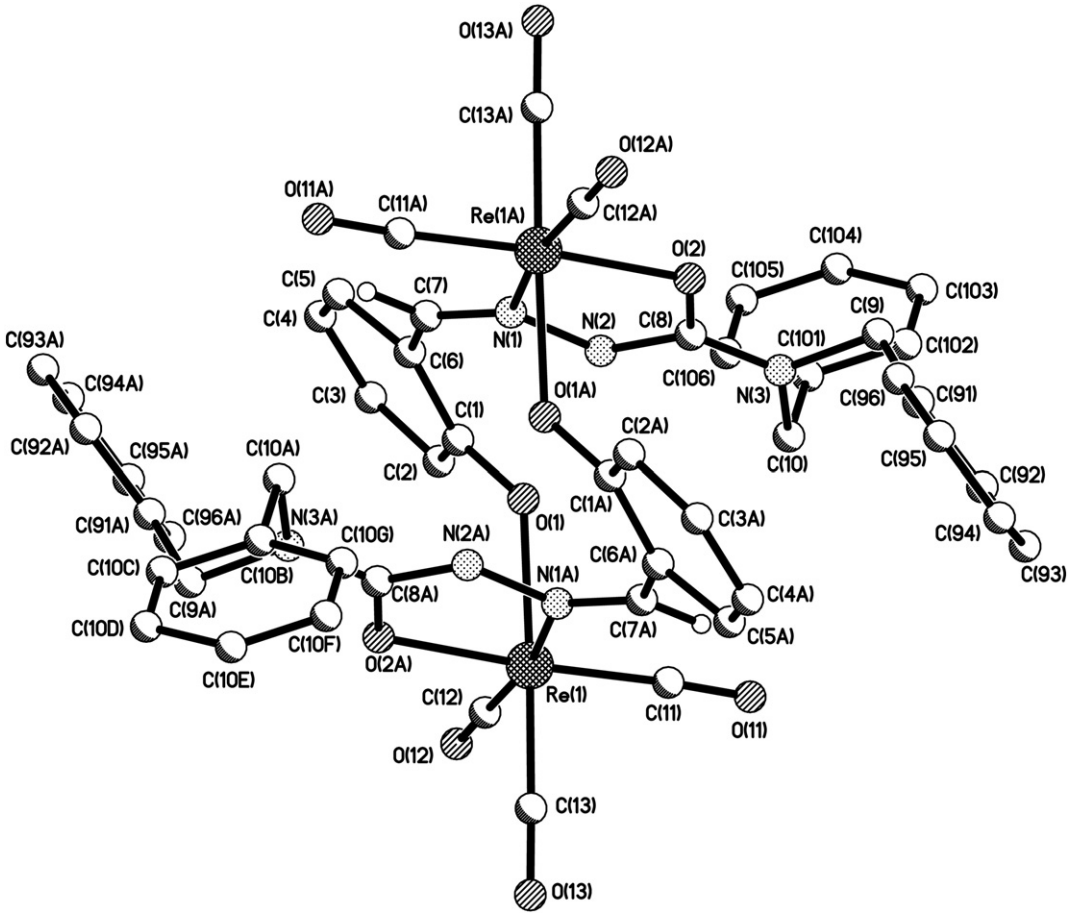

Fig. 5. Crystal structure of $[Re(CO)_3(HBnz_2)]_2$; all hydrogen atoms, except those of the imino groups [on C(7) and C(7A)], are omitted for clarity. The molecule has a crystallographic centre of symmetry.

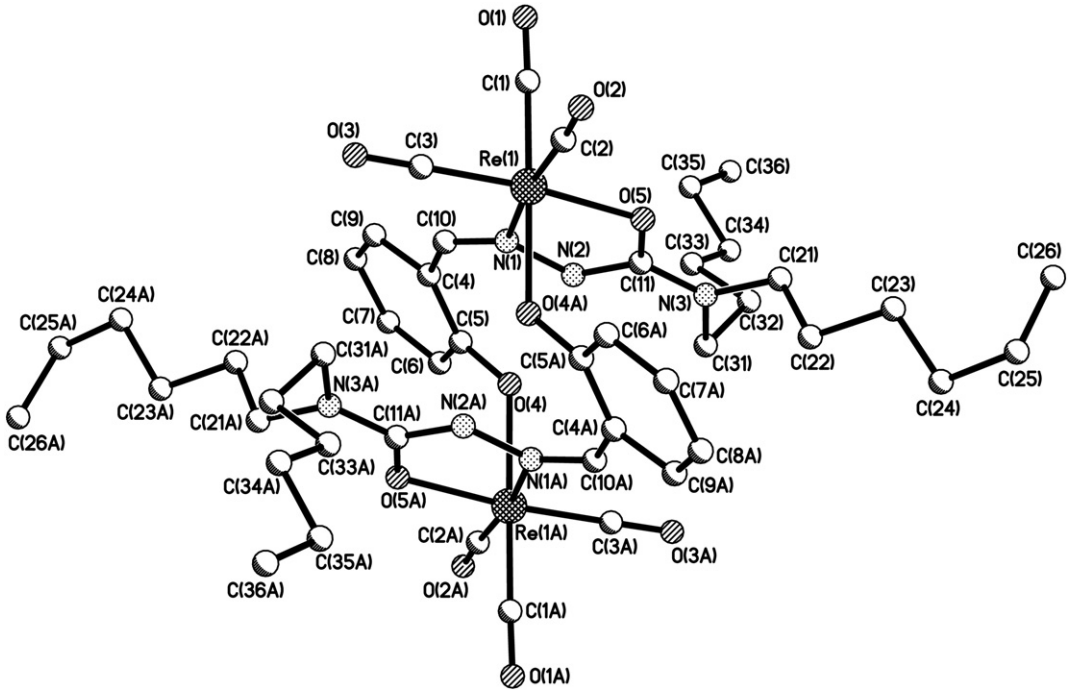

Fig. 6. Crystal structure of $[Re(CO)_3(HHex_2)]_2$; hydrogen atoms are omitted for clarity. The molecule has a crystallographic centre of symmetry.

Table 4
Selected bond lengths (Å) and angles (°) for $[Re(CO)_3(HBnz_2)]_2$ and $[Re(CO)_3(HHex_2)]_2$.

$[Re(CO)_3(HBnz_2)]_2$		$[Re(CO)_3(HHex_2)]_2$	
Bond lengths			
Re(1)-C(11)	1.909(7)	Re(1)-C(1)	1.899(8)
Re(1)-C(12)	1.911(6)	Re(1)-C(2)	1.925(8)
Re(1)-C(13)	1.904(6)	Re(1)-C(3)	1.897(8)
Re(1)-O(2A)	2.145(5)	Re(1)-O(5)	2.144(5)
Re(1)-N(1A)	2.189(4)	Re(1)-N(1)	2.190(5)
Re(1)-O(1)	2.158(4)	Re(1)-O(4A)	2.156(4)
C(7)-N(1)[a]	1.300(7)	C(10)-N(1)[a]	1.272(9)
C(8)-O(2)[b]	1.269(6)	C(11)-O(5)[b]	1.247(9)
C(8)-N(3)[c]	1.322(7)	C(11)-N(3)[c]	1.335(9)
C(8)-N(2)[d]	1.373(7)	C(11)-N(2)[d]	1.352(9)
Bond angles			
C(8)-N(3)-C(9)	118.5(5)	C(11)-N(3)-C(21)	119.9(6)
C(8)-N(3)-C(10)	123.9(5)	C(11)-N(3)-C(31)	123.4(6)
C(9)-N(3)-C(10)	117.3(5)	C(21)-N(3)-C(31)	116.7(5)

[a] Imine CN.
[b] Amide CO.
[c] Amide CN.
[d] Hydrazide CN.

centre and the phenoxo oxygen to the other. In general, the lengths of the C═O, C═N and C–N bonds within the SSC ligands (Table 4) do not differ significantly from those in $HOC_6H_4CH{=}N-NHCONH_2$ [34], although there is noticeable variation in the lengths of these bonds between $[Re(CO)_3(HBnz_2)]_2$ and $[Re(CO)_3(HHex_2)]_2$. Like those of $[ReBr(CO)_3(H_2Bu_2)]$, the amide nitrogens of both $[Re(CO)_3(HBnz_2)]_2$ and $[Re(CO)_3(HHex_2)]_2$ have trigonal planar coordination geometry (sum of bond angles = 360°). The imino protons of $[Re(CO)_3(HBnz_2)]_2$ and $[Re(CO)_3(HHex_2)]_2$ deviate more from the mean planes of the salicylaldehyde phenyl rings than those of $[ReBr(CO)_3(H_2Bu_2)]$, with the proton of $[Re(CO)_3(HBnz_2)]_2$ deviating by 0.41 Å and that of $[Re(CO)_3(HHex_2)]_2$ by 0.42 Å.

3.5. Cytotoxicity

The cytotoxicities of the SSCs and their rhenium tricarbonyl complexes were evaluated against MOLT-4 (cisplatin-sensitive [35]) and MCF-7 (cisplatin-resistant [36–38]) cells. To assess the selectivity of these compounds towards cancer cells, their cytotoxicities against fibroblasts (non-cancerous) were also determined. Cisplatin was included in the cytotoxicity assays for comparison. The results are shown in Table 5.

Generally, the $[ReBr(CO)_3(SSC)]$ complexes exhibit similar or higher activity than the corresponding SSC ligands against MOLT-4 cells, but are generally less active than the ligands against MCF-7 cells. The complexes $[ReBr(CO)_3(H_2Bnz_2)]$ and $[ReBr(CO)_3(H_2BF)]$ are the only ones with appreciable toxicity towards MCF-7 cells. They are also significantly more active than cisplatin against both MOLT-4 and MCF-7 cells.

Table 5
IC_{50} values of the SSC ligands and their rhenium carbonyl complexes. Standard errors are shown in parentheses (N = 6). The LogP values (logarithm of the partition coefficient between *n*-octanol and water) were calculated using the ChemDrawUltra 11.0 software.

Ligand (L)	LogP	IC_{50} (μM)					
		L			$[ReBr(CO)_3L]$		
		MOLT-4	MCF-7	Fibroblast	MOLT-4	MCF-7	Fibroblast
H_2MePh	2.59	56(3)	>125	>125	24(6)	>125	>125
H_2Ph_2	3.63	>63[a]	>63[a]	>63[a]	15(1)	>125	>125
H_2Bu_2	4.43	5(3)	5(4)	>125	15(1)	>125	>125
H_2Bnz_2	4.69	11(1)	8(3)	100(10)	7.3(0.4)	24 (4)	>125
H_2BF	5.02	[b]	[b]	[b]	1.0 (0.1)	35 (4)	9 (1)
H_2Hex_2	6.55	56(6)	8(4)	>125	22(2)	>125	>125
Cisplatin	–	18(1)	71(8)	28(2)	18(1)	71(8)	28(2)

[a] Highest concentration tested as the compound has poor solubility in the medium used for the cytotoxicity assay.
[b] Not soluble in the medium used for the cytotoxicity assay.

The cytotoxicity of the complexes towards MOLT-4 cells appears to be correlated with the lipophilicity of the ligands (Table 5). Cytotoxicity increases with increasing lipophilicity from H_2MePh to H_2Bnz_2/H_2BF, and decreases thereafter with a further increase in lipophilicity. This suggests that absorption across lipid membranes in the cells is an important factor determining the cytotoxicity of the compounds [39].

All the compounds tested except $[ReBr(CO)_3(H_2BF)]$ exhibit negligible toxicity against fibroblasts, showing that most of these compounds are selective against cancer cells. This is an important property for any chemotherapeutic agent, since harmful side effects of the treatment will be minimised. The complex $[ReBr(CO)_3(H_2Bnz_2)]$ stands out as the only one with appreciable activity against both MOLT-4 and MCF-7 cells, but negligible toxicity towards fibroblasts.

3.6. Solution chemistry

The solution chemistry of $[ReBr(CO)_3(H_2Bnz_2)]$ was investigated by ^1H NMR spectroscopy. This complex was chosen as it shows the best activity profile in the cytotoxicity assays. Since the solubility of $[ReBr(CO)_3(H_2Bnz_2)]$ in water is too low for NMR studies, investigations were conducted in $(CD_3)_2SO$.

The spectral changes that occurred after incubating a solution of $[ReBr(CO)_3(H_2Bnz_2)]$ at 37 °C for 24 h (Fig. 7) are consistent with the conversion of the compound to the dinuclear complex $[Re(CO)_3(HBnz_2)]_2$. In particular, signals attributed to the dinuclear complex (quartets at 4.54 and 6.78 ppm) appeared while those of the mononuclear complex (broad doublets at 4.43 and 4.64, triplet at 6.70, and doublet at 6.83 ppm) decreased in intensity. Since the quartet at 6.78 ppm overlaps with the doublet at 6.83 ppm but not the triplet at 6.70 ppm, the percent conversion of $[ReBr(CO)_3(H_2Bnz_2)]$ to $[Re(CO)_3(HBnz_2)]_2$ could be calculated to be about 50% from the expression $[(I_a - I_b)/(I_a + I_b)]$, where I_a is the total integrated intensity of the overlapping signals at 6.78 and 6.83 ppm and I_b is the integrated intensity of the triplet at 6.70 ppm. These observations are consistent with the facile conversion of $[ReBr(CO)_3(H_2Bnz_2)]$ to $[Re(CO)_3(HBnz_2)]_2$ during crystal growing experiments (Section 3.1).

To investigate the possible interaction of $[ReBr(CO)_3(H_2Bnz_2)]$ with DNA, we also examined the reaction of $[ReBr(CO)_3(H_2Bnz_2)]$ with guanosine. Addition of an equimolar amount of guanosine to a freshly-prepared solution of $[ReBr(CO)_3(H_2Bnz_2)]$ causes immediate changes to the ^1H NMR signals of $[ReBr(CO)_3(H_2Bnz_2)]$ (Fig. 8), most notably an upfield shift of the imine proton signal from 7.87 to 7.77 ppm and an upfield shift of the doublet at 6.83 ppm (assigned to the proton ortho to the hydroxyl group) to 6.78 ppm. These shifts are consistent with the deprotonation of the hydroxyl group of $[ReBr(CO)_3(H_2Bnz_2)]$. Correspondingly, the N(1)-H (10.63 ppm), C(8)-H (7.93 ppm) and NH_2 (6.46 ppm) signals of guanosine are shifted downfield to 10.98, 8.46 and ca. 6.7 ppm, respectively, indicating the protonation of guanosine, predominantly at N(7). Addition of 1.0, 6.7 and 13.4 molar equivalents of HCl (aq) to guanosine in $(CD_3)_2SO$ causes the chemical shift of C(8)-H to plateau at 9.33 ppm. Taking this to indicate 100% protonation of guanosine, the extent of protonation of guanosine observed in the presence of $[ReBr(CO)_3(H_2Bnz_2)]$ is calculated to be ca. 36%, assuming that the C(8)-H signal at 8.46 ppm is the weighted average of unprotonated and protonated guanosine. No change is observed for the C–H proton resonances of the ribose moiety [5.75, 4.39, 4.12 and 3.92 ppm for protons on C(1′)–C(4′), respectively; signals of protons on C(5′) are masked by the water peak], hence there is probably negligible interaction between the ribose unit and $[ReBr(CO)_3(H_2Bnz_2)]$.

Interestingly, no reaction was observed between guanosine and the free ligand, H_2Bnz_2, within 24 h, suggesting that H_2Bnz_2 is a much

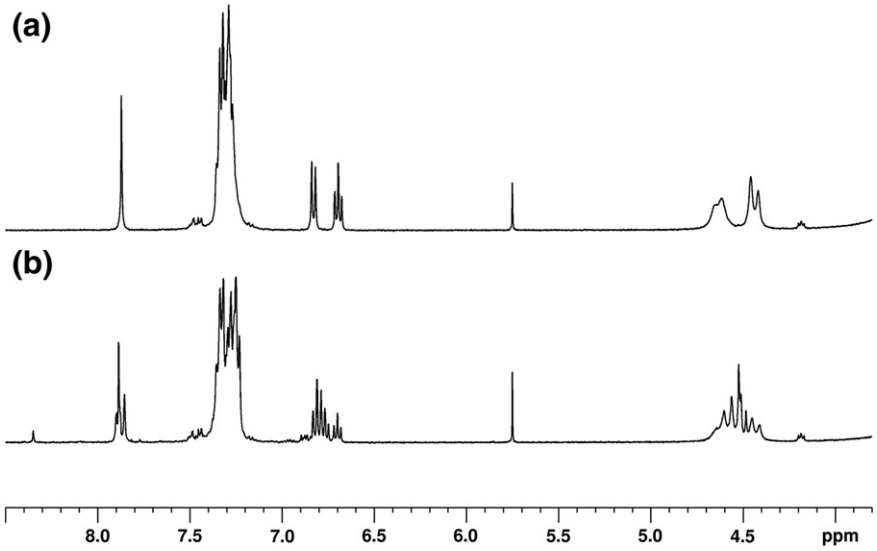

Fig. 7. Proton NMR spectra of $[ReBr(CO)_3(H_2Bnz_2)]$ (12 mM) in $(CD_3)_2SO$: (a) obtained from a freshly-prepared solution, (b) recorded after the solution was incubated at 37 °C for 24 h. The peak at 5.76 ppm is due to adventitious CH_2Cl_2.

weaker acid than $[ReBr(CO)_3(H_2Bnz_2)]$. The higher acid strength of $[ReBr(CO)_3(H_2Bnz_2)]$ may be due to the presence of an intramolecular (hydrazine)NH···O(phenol) hydrogen bond in the complex, assuming that hydrogen bonding similar to that observed in $[ReBr(CO)_3(H_2Bu_2)]$ (see Section 3.4.1) occurs in $[ReBr(CO)_3(H_2Bnz_2)]$. Intramolecular hydrogen bonding between phenolic oxygen atoms and NH protons is known to increase the acid strength of phenols [40]. The existence of the NH···O interaction is supported by the fact that the benzyl proton signals at 4.43 and 4.64 ppm shift upfield to 4.39 and 4.58 ppm, respectively (see Fig. 8), when guanosine is added to $[ReBr(CO)_3(H_2Bnz_2)]$: deprotonation of the phenolic oxygen increases the electron density on the hydrazine nitrogen, which increases the dominance of resonance structure IIb (Scheme 1) at the expense of structure IIa, thereby increasing the shielding of the benzyl protons. The $\{Re(CO)_3\}$ group probably also contributes to the higher acidity of the complex since the negative charge on the phenoxo oxygen can be delocalised onto the imino nitrogen, where it is stabilised by the Lewis acidic rhenium(I) centre.

Incubating the guanosine-$[ReBr(CO)_3(H_2Bnz_2)]$ mixture at 37 °C for 24 h resulted in the appearance of resonances due to $[Re(CO)_3(HBnz_2)]_2$ (Fig. 8). Taking the multiplet at 4.39 ppm to be composed of resonances of the guanosine C(2′)-H proton and two of the benzyl protons of $[ReBr(CO)_3(H_2Bnz_2)]$, and that at 4.54 ppm to be composed of resonances due to all four of the benzyl protons of $[Re(CO)_3(HBnz_2)]_2$ and two of the benzyl protons of $[ReBr(CO)_3(H_2Bnz_2)]$, the percent conversion of $[ReBr(CO)_3(H_2Bnz_2)]$ to $[Re(CO)_3(HBnz_2)]_2$ was calculated to be about 50% from the intensity ratio of the multiplets. The similar

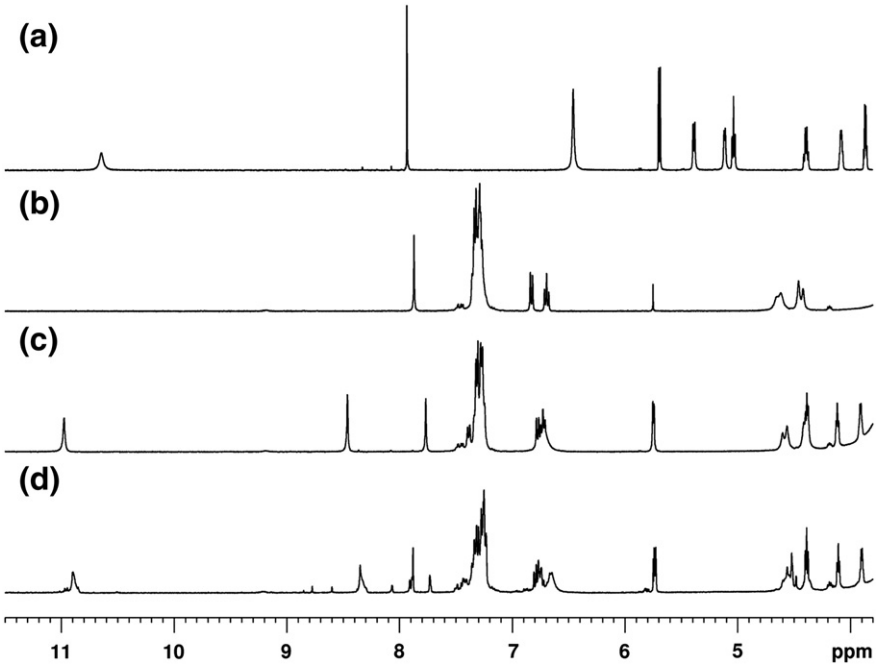

Fig. 8. Proton NMR spectra of: (a) guanosine, (b) $[ReBr(CO)_3(H_2Bnz_2)]$, (c) freshly-prepared mixture of guanosine and $[ReBr(CO)_3(H_2Bnz_2)]$, (d) guanosine-$[ReBr(CO)_3(H_2Bnz_2)]$ mixture incubated at 37 °C for 24 h. All solutes were dissolved in $(CD_3)_2SO$ at 12 mM concentration. The guanosine C(1′)-H signal overlaps with that of adventitious CH_2Cl_2 at 5.76 ppm.

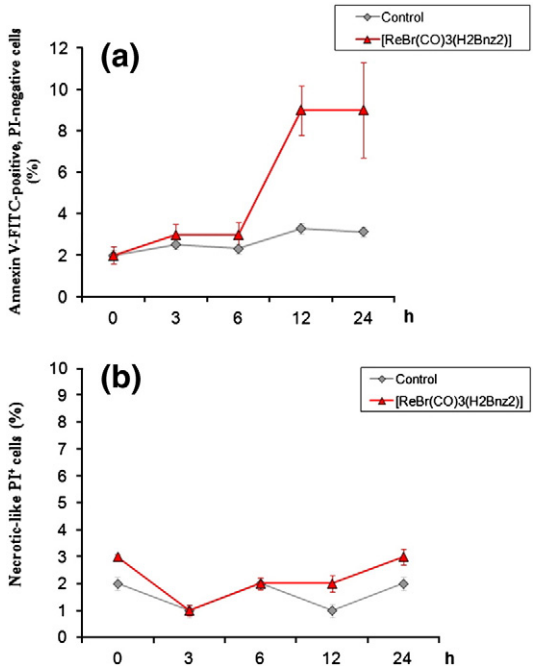

Fig. 9. Flow cytometric assessment of apoptosis in MOLT-4 cells treated with $[ReBr(CO)_3(H_2Bnz_2)]$ for 3, 6, 12 and 24 h, respectively: (a) cells stained with Annexin-V-FITC only; (b) cells stained with propidium iodide only.

percent conversion to that observed in the absence of guanosine is consistent with the earlier deduction (Section 3.1) that the rate-limiting step for dimerisation is bromide dissociation (and not deprotonation).

The relatively strong acidity of $[ReBr(CO)_3(H_2Bnz_2)]$ suggests that the deprotonated complex $[ReBr(CO)_3(HBnz_2)]^-$ is an important species interacting with cells during the cytotoxicity assay, while the facile formation of $[Re(CO)_3(HBnz_2)]_2$ suggests that bromide dissociation (i.e., solvolysis) occurs quite readily. It is unlikely for the dinuclear complex to be present in significant amounts in the cells, however, since its rate of formation would be negligible under conditions of high dilution in the assays. Hence, the unsaturated intermediate $[Re(CO)_3(H_2Bnz_2)]^+$ is likely to accept electron pairs from donor groups of biomolecules instead. The NMR spectra of $[ReBr(CO)_3(H_2Bnz_2)]$ and guanosine-$[ReBr(CO)_3(H_2Bnz_2)]$ mixture show no apparent signals assignable to uncomplexed H_2Bnz_2, hence ligand displacement does not occur to a significant extent within 24 h at 37 °C. Given that DMSO is a strong donor solvent, the lack of ligand displacement in DMSO suggests that ligand displacement is not involved in the mechanism of cytotoxicity of rhenium salicylaldehyde semicarbazone complexes.

3.7. Assessment of apoptosis induction by $[ReBr(CO)_3(H_2Bnz_2)]$

MOLT-4 cells treated with $[ReBr(CO)_3(H_2Bnz_2)]$ showed an increasing degree of Annexin-V-FITC positivity over time (Fig. 9), indicating that the cells were undergoing apoptosis. Occurrence of apoptosis was further confirmed by measuring the caspase 3 activity of treated cells. Activation of caspase 3 activity is integral to the initiation of apoptosis [41,42]. MOLT-4 cells treated with $[ReBr(CO)_3(H_2Bnz_2)]$ showed increased caspase 3 activity over the 24-h period of treatment (Fig. 10a), with activity reaching its maximum at 6 h. Correspondingly, western blotting with antibodies against caspase 3 also revealed the presence of an active cleaved 17 kDa caspase 3 subunit (Fig. 10b).

4. Summary and conclusion

A series of *N,N*-disubstituted salicylaldehyde semicarbazones (SSCs) and their rhenium(I) tricarbonyl complexes, $[ReBr(CO)_3(SSC)]$, have been synthesised and screened for cytotoxicity against MOLT-4, MCF-7 and human fibroblast cells. The dinuclear complexes, $[Re(CO)_3(HBnz_2)]_2$ and $[Re(CO)_3(HHex_2)]_2$, are formed during slow evaporation of dichloromethane-hexane solutions of $[ReBr(CO)_3(H_2Bnz_2)]$ and $[ReBr(CO)_3(H_2Hex_2)]$, respectively. Crystal structures have been determined for $[ReBr(CO)_3(H_2Bu_2)]$, $[Re(CO)_3(HBnz_2)]_2$ and $[Re(CO)_3(HHex_2)]_2$. On the whole, the

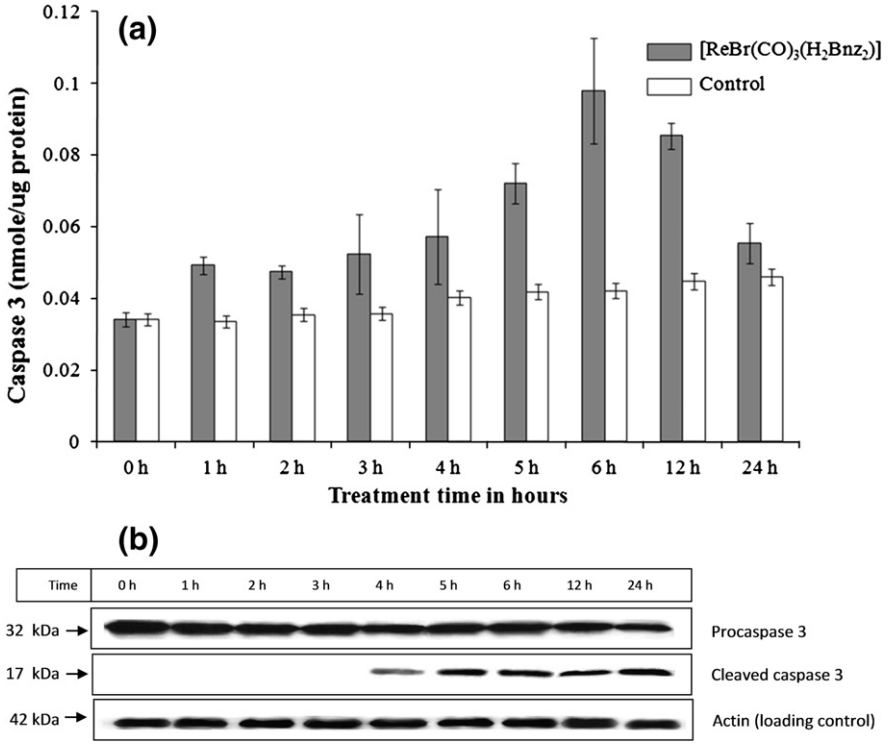

Fig. 10. Detection of caspase 3 activity in MOLT-4 cells treated with $[ReBr(CO)_3(H_2Bnz_2)]$: (a) colorimetric measurement of caspase-specific cleavage of Ac-DEVD-pNA; (b) western blot analysis of proteins separated by SDS-PAGE.

$[ReBr(CO)_3(SSC)]$ complexes exhibit similar or higher activity than the corresponding SSC ligands against MOLT-4 cells, with two complexes showing particularly high activities. Most of the tested compounds demonstrate negligible activity against non-cancerous fibroblasts. Of these compounds, $[ReBr(CO)_3(H_2Bnz_2)]$ shows the best cytotoxicity profile, being the only one that has high activity against both MOLT-4 and MCF-7 cells, and negligible toxicity towards fibroblasts. It also induces apoptosis in MOLT-4 cells. In $(CD_3)_2SO$, $[ReBr(CO)_3(H_2Bnz_2)]$ reacts with guanosine by proton transfer from the phenolic OH group to N(7) of guanosine. The relatively strong acidity of the OH group may be attributed to intramolecular (hydrazine) NH···O(phenol) hydrogen bonding, which is made possible by the adoption of the *cis* configuration by the imine group in $[ReBr(CO)_3(H_2Bnz_2)]$. Displacement of the SSC ligand is probably not involved in the mechanism of cytotoxicity of rhenium salicylaldehyde semicarbazone complexes, but interaction with biomolecules after loss of bromide is plausible.

Acknowledgements

The authors would like to thank Dr. Shu Uin Gan (Department of Surgery, National University of Singapore) for the provision of human fibroblasts. Financial support from the National Institute of Education, Singapore (grant number RI 4/05 LPF) is gratefully acknowledged. We also thank Ms. Ying-Chang Ting for the technical assistance.

Appendix A. Supplementary data

Crystallographic data (excluding structure factors) for the complexes $[ReBr(CO)_3(H_2Bu_2)]$, $[Re(CO)_3(HBnz_2)]_2$ and $[Re(CO)_3(HHex_2)]_2$ may be obtained from the Cambridge Crystallographic Data Centre (CCDC, 12 Union Road, Cambridge CB2 1EZ, UK; fax: _/44-1223-336-033; e-mail: deposit@ccdc.cam.ac.uk or www: http://www.ccdc.cam.ac.uk) on quoting the depository numbers CCDC 763433, 763434 and 763435, respectively.

Supplementary data to this article can be found online at doi http://dx.doi.org/10.1016/j.jinorgbio.2012.10.011.

References

[1] H. Beraldo, D. Gambino, Minirev. Med. Chem. 4 (2004) 31–39.
[2] A. Quiroga, C. Ranninger, Coord. Chem. Rev. 248 (2004) 119–133.
[3] Z. Afrasiabi, E. Sinn, W. Lin, Y. Ma, C. Campana, S.B. Padhyé, J. Inorg. Biochem. 99 (2005) 1526–1531.
[4] Z. Afrasiabi, E. Sinn, S. Padhye, S. Dutta, C. Newton, C.E. Anson, A.K. Powell, J. Inorg. Biochem. 95 (2003) 306–314.
[5] R.W. Byrnes, M. Mohan, W.E. Antholine, R.X. Xu, D.H. Petering, Biochemistry 29 (1990) 7046–7053.
[6] I.H. Hall, S.Y. Chen, B.J. Barners, D.X. West, Metal-Based Drugs 6 (1999) 143–147.
[7] D.L. Klayman, J.F. Bartosovich, T.S. Griffin, C.J. Mason, J.P. Scovill, J. Med. Chem. 22 (1979) 855–862.
[8] R.C. Condit, R. Easterly, R.F. Pacha, Z. Fathi, R.J. Meis, Virology 185 (1991) 857–861.
[9] M. Belicchi-Ferrari, F. Bisceglie, G. Pelosi, P. Tarasconi, Polyhedron 27 (2008) 1361–1367.
[10] M. Baldini, M. Belicchi-Ferrari, F. Bisceglie, G. Pelosi, S. Pinelli, P. Tarasconi, Inorg. Chem. 42 (2003) 2049–2055.
[11] M. Belicchi-Ferrari, F. Bisceglie, C. Casoli, S. Durot, I. Morgenstern-Badara, G. Pelosi, E. Pilotti, S. Pinelli, P. Tarasconi, J. Med. Chem. 48 (2005) 1671–1675.
[12] M. Belicchi-Ferrari, G. Gasparri-Fava, E. Leporati, G. Pelosi, R. Rossi, P. Tarasconi, R. Albertini, A. Bonati, P. Lunghi, S. Pinello, J. Inorg. Biochem. 70 (1998) 145–154.
[13] M. Belicchi-Ferrari, F. Bisceglie, G. Pelosi, P. Tarasconi, R. Albertini, A. Bonati, P. Lunghi, S. Pinelli, J. Inorg. Biochem. 83 (2001) 169–179.
[14] Z. Afrasiabi, E. Sinn, J. Chen, Y. Ma, A.L. Rheingold, L.N. Zakharov, Inorg. Chim. Acta 357 (2004) 271.
[15] N.C. Kasuga, K. Sekino, M. Ishikawa, A. Honda, M. Yokoyama, S. Nakano, N. Shimada, C. Koumo, K. Nomiya, J. Inorg. Biochem. 96 (2003) 298–310.
[16] C.R. Kowol, R. Berger, R. Eichinger, A. Roller, M.A. Jakupec, P.P. Schmidt, V.B. Arion, B.K. Keppler, J. Med. Chem. 50 (2007) 1254–1265.
[17] J. Patole, S. Padhye, M.S. Moodbidri, N. Shirsat, Eur. J. Med. Chem. 40 (2005) 1052–1055.
[18] U.K. Mazumder, M. Gupta, S.S. Karki, S. Bhattacharya, S. Rathinasamy, S. Thangavel, Chem. Pharm. Bull. 52 (2004) 178–185.
[19] S. Grguric-Sipka, C.R. Kowol, S.-M. Valiahdi, R. Eichinger, M.A. Jakupec, A. Roller, S. Shova, V.B. Arion, B.K. Keppler, Eur. J. Inorg. Chem. (2007) 2870–2878.
[20] P. Noblia, E.J. Baran, L. Otero, P. Draper, H. Cerecetto, M. Gonzalez, O.E. Piro, E.E. Castellano, T. Inohara, Y. Adachi, H. Sakurai, D. Gambino, Eur. J. Inorg. Chem. (2004) 322–328.
[21] W.Y. Lee, P.P.F. Lee, Y.K. Yan, M. Lau, Metallomics 2 (2010) 694–705.
[22] J. Rivadeneira, D.A. Barrio, G. Arrambide, D. Gambino, L. Bruzzone, S.B. Etcheverry, J. Inorg. Biochem. 103 (2009) 633–642.
[23] J. Zhang, J.J. Vittal, W. Henderson, J. Wheaton, I.H. Hall, T.S. Hor, Y.K. Yan, J. Organomet. Chem. 650 (2002) 123–132.
[24] W. Wang, Y.K. Yan, T.S. Hor, J.J. Vittal, J.R. Wheaton, I.H. Hall, Polyhedron 21 (2002) 1991–1999.
[25] A. Nunez-Montenegro, R. Carballo, E.M. Vazquez-Lopez, Polyhedron 27 (2008) 2867–2876.
[26] G. Pereiras-Gabian, E.M. Vazquez-Lopez, U. Abram, Z. Anorg. Allg. Chem. 630 (2004) 1665–1670.
[27] R. Carballo, J.S. Casas, E. Garcia-Martinez, G. Pereiras-Gabian, A. Sanchez, J. Sordo, E.M. Vazquez-Lopez, J.C. Garcia-Monteagudo, U. Abram, J. Organomet. Chem. 656 (2002) 1–10.
[28] I.G. Santos, U. Abram, R. Alberto, E.V. Lopez, A. Sanchez, Inorg. Chem. 43 (2004) 1834–1836.
[29] S.P. Schmidt, W.C. Trogler, F. Basolo, Inorg. Synth. 28 (1990) 160–165.
[30] P.F. Lee, C.T. Yang, D. Fan, J.J. Vittal, J. Ranford, Polyhedron 22 (2003) 2781–2786.
[31] M.B. Hansen, T. Fojo, J. Immunol. Methods 119 (1989) 203–210.
[32] J.F. Kerr, A.H. Wyllie, A.R. Currie, Br. J. Cancer 26 (1972) 239–257.
[33] I. Vermes, C. Haanen, H. Steffens-Nakken, C. Reutelingsperger, J. Immunol. Methods 184 (1995) 39–51.
[34] J. Valdes-Martinez, R.A. Toscano, R. Salcedo, R. Cea-Olivares, A. Melendez, Monatsh. Chem. 121 (1990) 641–647.
[35] D.M. Fan, C.T. Yang, J.D. Ranford, J.J. Vittal, P.F. Lee, J. Chem. Soc. Dalton Trans. (2003) 2680–2685.
[36] W. Friebolin, G. Schilling, M. Zoller, E. Amtmann, J. Med. Chem. 48 (2005) 7925–7931.
[37] Y.J. Chua, C. Steer, D. Yip, Cancer Treat. Rev. 30 (2004) 521–543.
[38] F.M. Muggia, T. Fojo, J. Chemother. 16 (Suppl. 4) (2004) 77–82.
[39] C.A. Lipinski, F. Lombardo, B.W. Dominy, P.J. Feeney, Adv. Drug Deliv. Rev. 46 (2001) 3–26.
[40] D. Kanamori, A. Furukawa, T. Okamura, H. Yamamoto, N. Ueyama, Org. Biomol. Chem. 3 (2005) 1453–1459.
[41] Z. Tao, J. Goodisman, H.S. Penefsky, A.K. Souid, Mol. Pharm. 4 (2007) 583–595.
[42] N.A. Thornberry, Y. Lazebnik, Science 281 (1998) 1312–1316.